TABLE I The output of an indexing system from the program. The first column gives the measured distances, R, on the diffraction pattern, the next column gives the reciprocal lattice vector, g, corresponding to R using the given λL value. g_{calc} gives the corresponding vector magnitude from the reciprocal lattice, which is followed by the Miller indices of the corresponding plane in the direct lattice. The next column gives the difference ($g - g_{calc}$) and is followed by the λL value deduced from g_{calc}. This gives an idea of the measuring errors for the three R values, in the scatter in λL. Finally the angles measured and calculated are listed, together with an identifier, e.g. (1-2) means the angle between the first and second R.
Given $\lambda L = 14.4 \pm 2\%$

R	g	g_{calc}	Indices			$g - g_{calc}$	λL	Angle	
								Measured	Calculated
1.70	0.118	0.1194	1	−1	0	0.001	14.24	103.2	104.1 (1-2)
2.80	0.194	0.1959	−1	0	1	0.001	14.29	69.0	69.6 (1-3)
2.91	0.202	0.2024	0	1	1	0.000	14.38	34.4	34.8 (2-3)

plane, the problem is even worse, since the reflections are then streaked obliquely across the plane of the pattern and the reflection may occur well away from the reciprocal lattice point. To improve this situation, operators should tilt the foils to the position where the intensity of the reflection is maximized before recording the pattern in such cases.

In the program described here, the operator is required to indicate error limits for both types of errors and the output gives an estimate of the actual error found. The two types of error are used differently since one (λL) behaves as a uniform scaling factor for the whole pattern while the other varies from one reflection to the next.

The program itself is included in a booklet which gives full details of its operation. It is written in standard (ANSI) Fortran and uses a method of computation described previously [1]. The user provides three (or fewer) measured distances to reflections on the pattern and the angles between them. The camera constant and the two error limits are also required. The program uses these data to produce three reciprocal lattice vectors which are then compared for size and for the angles between them, with the three-dimensional reciprocal lattice obtained from the structural data provided by the user.

When a suitable fit to three co-planar vectors has been obtained, the output produced is shown in Table I. The search is then continued until all possible indexing systems have been output.

In the event of a failure to index a pattern to the given structure ample fault messages are given to explain why. The efficiency of the computation is indicated by the fact that the CDC 7600/ICL 1906 combined machine at Manchester completes a single indexing in 0.25 sec.

Reference

1. M. BOOTH, M. GITTOS, and P. WILKES, *Met. Trans.* February 1974.

Received and accepted
9 November 1973

P. WILKES
Department of Metallurgy,
University of Manchester, UK

Lead-induced discontinuous precipitation in Fe-Au

In a recent review, the phenomena that occur in connection with discontinuous precipitation were discussed systematically [1]. It was noted that heat-treatments in specific environments may induce discontinuous precipitation in alloys which do not normally exhibit this reaction for any alloy compositions or ageing temperatures. In the following, this effect will be substantiated by reporting results on the precipitation reactions which occur in Fe-Au alloys aged in liquid Pb.

The system Fe-Au is characterized by a miscibility gap between the bcc or fcc iron-rich and the fcc gold-rich solid solutions. Fcc gold particles may be nucleated heterogeneously at dislocations or homogeneously in the supersaturated α-Fe-Au solid solutions [2, 3]. The

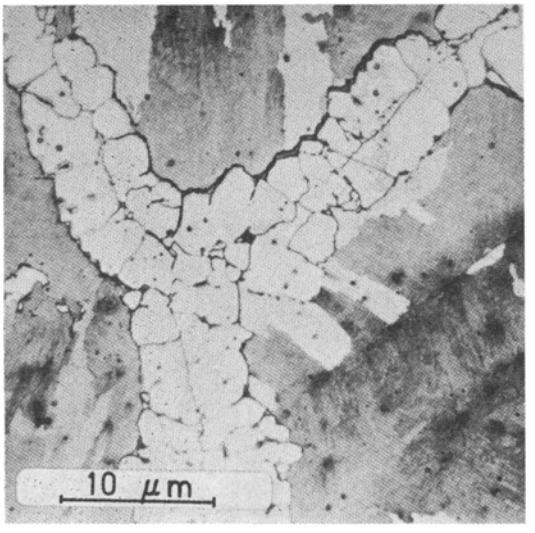

Figure 1 Fe-3.8 at % Au, quenched from 1000°C and aged 24 h at 500°C in Pb; discontinuous precipitation starts at grain boundaries (light microscopy).

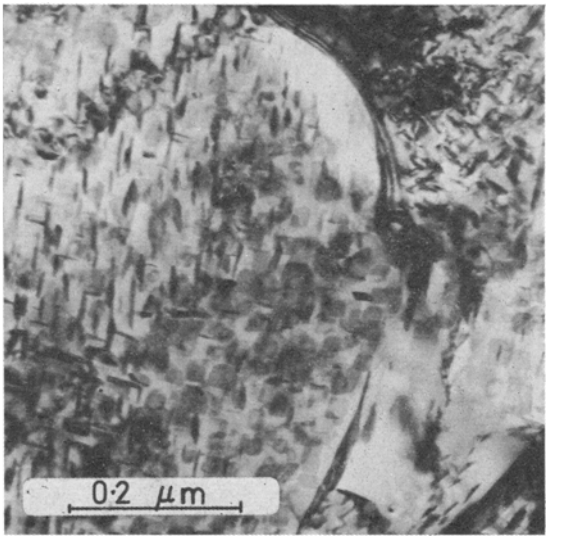

Figure 3 Fe-3.8 at % Au, aged 10 min at 600°C in Pb; continuous precipitation of gold, discontinuous precipitation has not yet started.

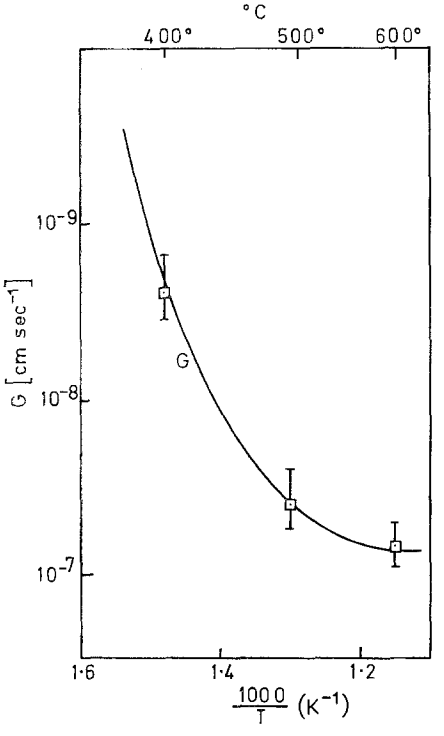

Figure 2 Temperature dependence of the velocity of the reaction front G, as obtained by light microscopy.

following results are obtained if these alloys (1.1 and 3.8 at. % Au) are aged between 400 and 600°C in liquid lead (Fig. 1).

A reaction front develops at the grain boundaries which advances through the alloy at an approximately constant velocity G. This velocity decreases with decreasing temperature, as shown in Fig. 2, and the normal precipitation of plate-like gold particles takes place ahead of the reaction front (Fig. 3). A second reaction is initiated at the grain boundaries, which move segmentally in one direction. In the reaction front, the gold particles are dissolved and a new phase is formed:

$$\alpha\text{-Fe(Au)} + \gamma\text{-Au(Fe)} \rightarrow \alpha\text{-Fe(Au)}^* + \mathrm{Pb}_x\mathrm{Au}_y\mathrm{Fe}_z\,.$$

From the contrast in the transmission micrographs, it may be deduced that the gold content of the α-Fe(Au) solid solution is decreased (Fig. 4). The new phase always forms in connection with the moving reaction front. The particles sometimes form as lamellae with a spacing of 1.0 μm (Fig. 4c) but in general are irregularly shaped, as a result of becoming detached from the reaction front. From the contrast, it may be deduced that the heavy atoms are concentrated in this phase. A determination of the crystal structure of this phase was attempted and a pattern obtained which indicated a very large unit cell which could not be identified unambiguously.

The reaction must have been induced by lead

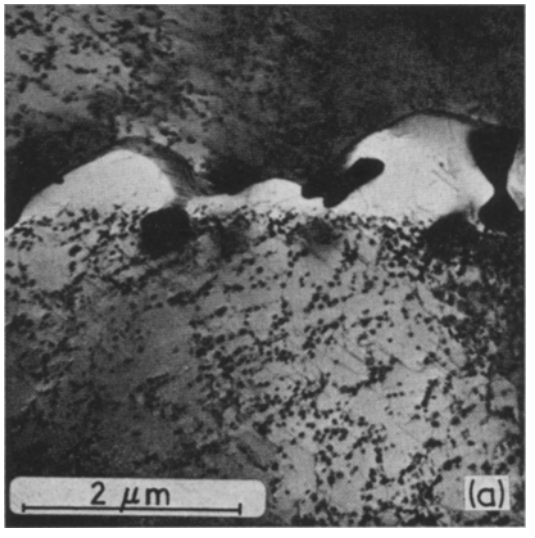

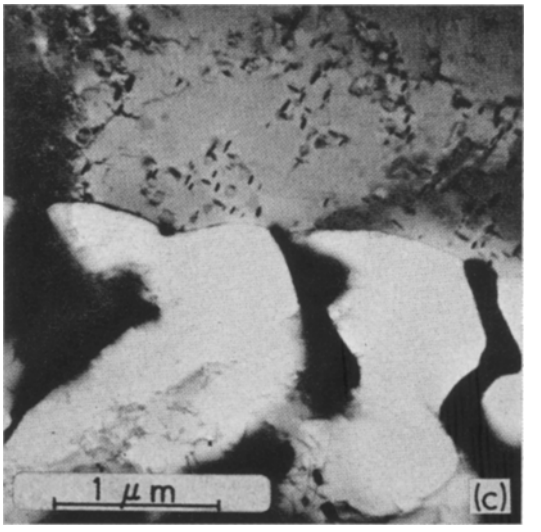

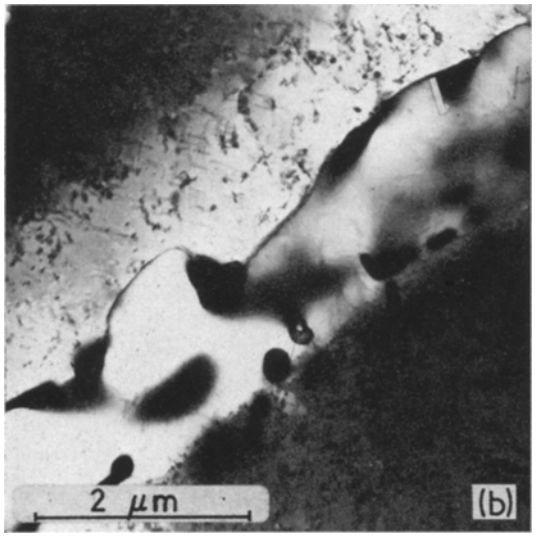

Figure 4 Fe 1.1 at. % Au, aged 5 h at 600°C in Pb, different sites in one specimen. (a) The discontinuous reaction is indicated by the movement of the grain boundary in one direction. The gold particles are dissolved and large particles of the new compound are formed in contact with the boundary. (b) On further motion of the boundary, the particles become detached from the growth front. (c) Formation of lamellae.

moving into the iron via the grain boundaries. Because of the complete immiscibility between solid Fe and Pb, this can only be facilitated by Au atoms segregated at the boundaries. Pb and Au form several intermetallic compounds that all melt below 420°C. Therefore, an unknown ternary compound $Pb_xAu_yFe_z$ must exist, if the compound is solid at its formation temperature. There was no difference in the thickness of the decomposed zone at grain boundaries over the cross-section of specimens 1 to 2 mm thick. This indicates that a very high grain-boundary diffusity, D_B, must be effective. From the measurements of reaction velocity, G, D_B cannot be calculated accurately because the supersaturation $\ln(c_o/c_e)$ is not known. However, an order of magnitude estimate for D_B may be made. In a specimen of a thickness $S = 0.2$ cm, the reaction started after about $t = 1$ h at 600°C. The lead which usually does not enter the iron must have penetrated a distance of 0.1 cm.

$$D_{600°C} \leqq \frac{s^2}{8t} \lesssim 10^{-6} \text{ cm}^2 \text{ sec}^{-1} . \quad (1)$$

This indicates that a diffusion coefficient a little less than that of liquid Pb is effective in the grain boundaries. This value can be used in the equation that relates growth velocity, G, lamellar spacing, S_L, and the thickness of this reaction front to estimate the effective supersaturation $\ln (c_o/c_e)$.

$$G = \ln \frac{c_o}{c_e} \frac{D_B \lambda}{8 S_L^2} , \quad (2)$$

with $G = 10^{-7}$ cm sec^{-1}, $\lambda = 4 \times 10^{-8}$ cm, $S_L = 3 \times 10^{-4}$ cm at 600°C, a value of $\ln c_o/c_e < 1$ is obtained which is smaller than expected.

Therefore, a value of $D_{B600°C} \gg 10^{-6}$ cm^2 sec^{-1} must control the diffusion of lead into the iron.

The results indicate that relatively small amounts of certain second elements can change grain-boundary diffusity to a large extent. Discontinuous precipitation is induced, if a more stable compound can be formed with the atoms which have penetrated through the surface. This process is likely to be of some practical importance, because lead-induced failures have already been reported in high strength steels [4]. It is not known as yet which other alloying elements in steels will produce similar effects.

References

1. E. HORNBOGEN, *Met. Trans.* **3** (1972) 2717.
2. *Idem, Acta Metallurgica* **10** (1962) 1187.
3. E. HORNBOGEN and M. ROTH, *Arch. Eisenhüttenw.* **36** (1965) 201.
4. N. N. BREYER and P. GORDON, in "The Microstructure and Design of Alloys" (The Institute of Metals and The Iron and Steel Institute, Cambridge, 1973) p. 493.

Received 19 November
and accepted 26 November 1973

E. HORNBOGEN
Institut für Werkstoffe,
Ruhr-Universität Bochum,
Germany

Improved "single-crystal" texture in high-density polyethylene

Any study of the relation between structure and physical properties of crystalline polymers is greatly facilitated by using a material with as single and well-defined a texture as possible. In studies on high density bulk polyethylene it has been established that suitable combinations of deformation and heat-treatment can result in an oriented polycrystalline sample with a texture resembling that of a single crystal [1-9]. The degree of orientation obtained depends on the method used, and to date one of the most successful techniques for this has been the combination of compression-orienting followed by high pressure annealing [6, 8]. The purpose of this note is to report a modification of the above technique which has further improved the polyethylene texture.

The material used in this investigation was injection-moulded high density polyethylene (Rigidex 9) supplied in the form of granules by British Petrochemicals Limited. The material was oriented and annealed using similar apparatus to that described earlier [6], but thermistor-controlled heaters were added to the compression dies so that material could be compressed at elevated temperatures. The injection-moulded bar was first compression-oriented at 110 $\pm$ 2°C and then annealed for 15 min at 207 $\pm$ 3°C and 4 kbar pressure. The material was initially 12.5 mm thick and at the end of the process was 0.5 mm (thickness reduction of 25 times). Wide-angle X-ray photographs revealed that prior to annealing, the compression oriented material had a good "single-crystal' texture of orthorhombic polyethylene, but there were also reflections indicating the presence of some monoclinic polyethylene. Subsequent pressure-annealing removed the monoclinic phase but also caused a slight reduction in the degree of crystallographic orientation in the specimen.

The final texture was examined by taking wide-angle pole figures using the diffractometer technique described earlier [10]. The combined

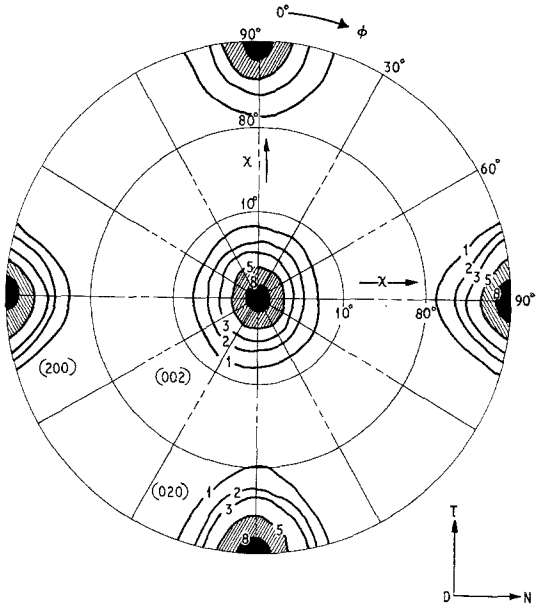

Figure 1. Combined wide-angle pole figures for the (200), (020) and (002) poles for hot compressed/pressure-annealed high density polyethylene.